J Nanostruct Chem (2016) 6:223–233
DOI 10.1007/s40097-016-0196-z

ORIGINAL RESEARCH

Synthesis and properties of magnetite/hydroxyapatite/doxorubicin nanocomposites and magnetic liquids based on them

N. V. Abramov[1] · S. P. Turanska[1] · A. P. Kusyak[1,2] · A. L. Petranovska[1] · P. P. Gorbyk[1]

Received: 21 March 2016 / Accepted: 12 May 2016 / Published online: 27 May 2016

Abstract Core–shell magnetosensitive nanocomposites (NC) based on single-domain magnetite (Fe_3O_4, core), with a shell consisting of hydroxyapatite (HA) and cytotoxic drug doxorubicin (DOX) layers have been synthesized. The processes of DOX adsorption on Fe_3O_4/HA surface from physiologic solution have been studied. DOX release into saline was found to decrease with growing of its quantity on NC surface. It has been determined that cytotoxic influence and antiproliferative activity of Fe_3O_4/HA/DOX NC with respect to *Saccharomyces cerevisiae* cells are characteristic for interaction of these cells with a free form of doxorubicin. Magnetic liquids containing Fe_3O_4/HA/DOX NC stabilized by sodium oleate and polyethylene glycol were prepared and investigated. It is shown that using the ensemble of Fe_3O_4 carriers as a superparamagnetic probe, the Langevin's paramagnetism theory, and the values of density of nanocomposite constituents, one can evaluate the size parameters of their shell, which has been corroborated by independent measurements of specific surface area of nanostructures and kinetic stability of the corresponding magnetic liquids. The obtained results may be useful for development and optimization of novel forms of magnetocarried medical remedies of targeted delivery and adsorbents based on nanocomposites of superparamagnetic core–shell type with multilevel nanoarchitecture, as well as for determination and control of the size parameters of its components.

Keywords Magnetite · Doxorubicin adsorption · Magnetite/hydroxyapatite/doxorubicin nanocomposites · Magnetic liquids · Dry residues · Size parameters of nanostructure

Introduction

Magnetic nanoparticles are widely used for the preparation of novel multifunctional therapeutic and diagnostic agents for different fields of medicine [1–3], including oncology. Conjugation of nanoparticles with corresponding antibody provides nanoparticles with the ability to recognize and "mark" specific microbiological objects, cell populations, microorganisms, and so on. On this basis, the concept has been substantiated for chemical construction of magnetosensitive nanocomposites with multilevel hierarchical architecture, characterized with functions of "nanoclinics" [2] and biomedical nanorobots [3–5] (recognition of microbiological objects in biological environments; the aimed delivery of drugs to target cells and organs using an external magnetic field and deposition; complex chemo-, immuno-, neutron capture, real-time hyperthermic therapy and diagnostics).

To produce magnetosensitive multifunctional nanocomposites (NC), considerable interest of researchers is drawn by magnetite (Fe_3O_4)/hydroxyapatite (HA) nanostructures of core–shell type, characterized with a unique set of physical, chemical, and biological properties, the ability to create on their basis magnetic liquids (ML) containing anticancer remedies for different functional destination, including cytotoxic drug, anthracycline

✉ P. P. Gorbyk
phorbyk@ukr.net

[1] Chuiko Institute of Surface Chemistry, National Academy of Sciences of Ukraine, 17 General Naumov Str., Kiev 03164, Ukraine

[2] Ivan Franko Zhytomyr State University, 40V. Berdychevska Str., Zhytomyr 10008, Ukraine

antibiotic doxorubicin (DOX) [6–17]. In this regard, the urgent task is to study the characteristics of the processes of adsorptive immobilization of DOX on the surface of Fe_3O_4/HA nanocomposites and its release into the saline, which is used to create ML for medical purposes, while maintaining biological activity of the cytotoxic drug.

It has been shown [18] that for a magnetite-based polydisperse colloidal ML the coordination of experimental and theoretical magnetization curves is possible when assuming that Fe_3O_4 particles have complex magnetic structure, namely, a low-magnetic surface layer with thickness $h_1 \sim 0.83$ nm (the lattice constant of magnetite at 300 K is 0.824 nm). Emergence of the said layer is attributed to chemical interaction of a particle with a stabilizing surfactant [19]. In [11, 20], it was found that the calculations of magnetization curve for ML based on single-domain Fe_3O_4 in the framework of Langevin's paramagnetism theory coordinate satisfactorily with the experimental results in assumption that saturation magnetization of magnetite particles depends on their sizes, and from experimentally measured distributions of the nanoparticles in ensemble one can calculate the magnetization curve for ML based on them.

An important issue is to find the size distribution for ensemble of superparamagnetic nanoparticles with complex shell structure from experimental measurements of the magnetization curve. Its successful resolution could open the way for determination of size parameters of nanoarchitecture elements that make multicomponent shell structure of the nanocomposite, built on superparamagnetic nanosized carriers, including those in the composition of magnetic liquids.

Therefore, from the above, it can be argued that investigations of the possibility of using approaches applied in [11, 20], based on the use of Langevin's paramagnetism theory, for the description of nanocomposites with superparamagnetic cores and complex shell structures of different chemical nature and magnetic liquids based on them, are urgent.

The aim of this work is to investigate the DOX adsorption on the surface of magnetite/hydroxyapatite nanostructures, to synthesis bioactive nanocomposites magnetite/hydroxyapatite/doxorubicin of core–shell type and ML based on them, to study the magnetic properties of nanocomposites and liquids, to analyze the results using Langevin's paramagnetism theory, and to determine the size parameters of multicomponent shell structure of the nanocomposites.

Experimental

Synthesis of initial magnetite, magnetite/hydroxyapatite nanocomposites, their properties and parameters, doxorubicin adsorption calculation technique are described in [11]. In this work, we used Fe_3O_4 and Fe_3O_4/HA samples with the specific surface area $S_{sp} \sim 110$ and 100 ± 5 % m^2/g, respectively. Presence of HA shell did not practically change the magnetic properties [21] of initial magnetite (the nanocomposite core).

Investigation of nanomaterials biocompatibility was carried out by studying their influence on cell viability of baker's yeast *Saccharomyces cerevisiae* [22, 23] with the help of Goryaev chamber using optical microscopy (biological microscope of Bresser Erudit type), and methylene blue dye by registration of concentration change for cells growing at the temperature of 22 °C in suspensions containing nanocomposites, yeast cells, minimal synthetic nutrient medium (MSM) [24], saline (PS). Numerically viability (K) was evaluated by the formula: $K = M_1/(M_1 + M_2) \times 100$ %, where M_1 is a number of living cells, M_2 is a number of dead cells. The data obtained was compared to the results of control samples studies.

Bioactivity of NC Fe_3O_4/HA modified with DOX was evaluated from their cytotoxic influence on *S. cerevisiae* cells [25, 26] and a decrease in cell proliferation rate [24]. These effects are, in particular, due to participation of doxorubicin in redox cyclic reactions and a corresponding increase in quantity of free radical molecules, to induction of oxidative stress, and to cell cycle delay in G_1- and S-phase. The concentration of cells (n, mL^{-1}) was calculated by the formula of Goryaev chamber: $n = N \times 2.5 \times 10^5$, where N is a number of cells above a large square of the chamber.

Investigation of isotherm of DOX adsorption on the surface of Fe_3O_4/HA NC was performed as follows. Samples (g) of Fe_3O_4/HA NC of 30 mg were mixed with DOX solutions ($V = 5$ mL) of different concentration. DOX adsorption was carried out in saline (PS) for 2 h in dynamic mode at room temperature and pH = 7.0. The quantity of the substance adsorbed on the surface of nanocomposites was determined by measuring DOX concentration in the contact solutions before and after adsorption. The concentration was measured with the help of a spectrophotometer Spectrometer Lambda 35 UV/Vis Perkin Elmer Instruments at $\lambda = 480$ nm using a calibration graph. In this work the lyophilized preparation DOXORUBICIN-TEVA (Pharmachemie BV, The Netherlands) was used.

To study the time dependences of DOX adsorption on the surface of Fe_3O_4/HA NC, as well as to study the isotherms, we used the samples (30 mg) of Fe_3O_4/HA nanocomposite, which were mixed with DOX solutions in saline ($V = 5$ mL) of varying concentration, DOX adsorption was carried out in dynamic regime using a shaker at room temperature. The quantity of the substance adsorbed on the surface of nanocomposites was determined by measuring DOX concentration in contact solutions in fixed time (from 30 min to 24 h).

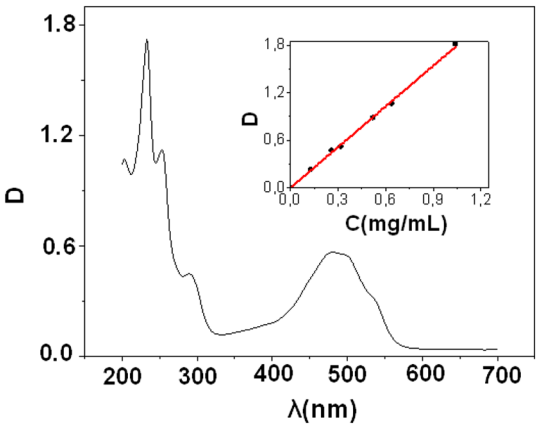

Paint (Word)

Fig. 1 Absorption spectrum of doxorubicin in PS environment. **a** Calibration graph

Calculation of the hydroxyl groups concentration on the HA surface in Fe_3O_4/HA nanocomposite was determined by thermogravimetric analysis using a derivatograph Q-1500.

Results and discussion

Adsorption studies

Doxorubicin [27] is the antitumor antibiotic agent of anthracycline type, widely used in modern oncotherapy. The mechanism of action is interaction with DNA, formation of free radicals, and direct influence on cell membranes with suppression of nucleic acids synthesis. It is characterized by an appreciable antiproliferative effect.

The DOX absorption spectrum measured in a physiological liquid environment is shown in Fig. 1.

The spectrum has several maxima: 204, 233, 254, 290, 480 cm^{-1}, a slope angle of the line of calibration graph for doxorubicin in the saline environment was optimal for the wavelength $\lambda = 480$ nm (Fig. 1a), at which we carried out the quantitative measurements of doxorubicin concentration.

Analysis of the isotherm of DOX adsorption on the surface of Fe_3O_4/HA NC (Fig. 2) shows that increase in equilibrium DOX concentration does not lead to adsorption saturation of the surface of Fe_3O_4/HA adsorbent. Concavity (S-similarity) of an initial part of isotherm relatively to the concentration axis and lack of saturation in the investigated range of equilibrium concentrations can be attributed to the polymolecular nature of adsorption and low porosity of the nanocomposite surface. In addition, S-similarity of isotherm can be caused to some extent by co-adsorption of sodium chloride because DOX adsorption was performed from saline.

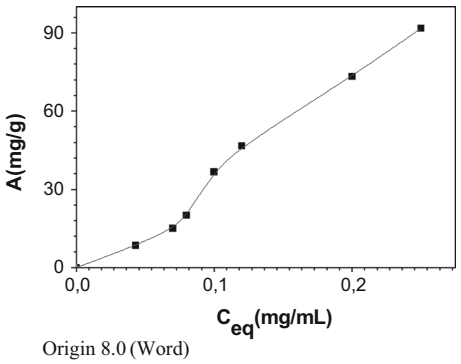

Origin 8.0 (Word)

Fig. 2 Isotherm of doxorubicin adsorption on the surface of Fe_3O_4/HA NC

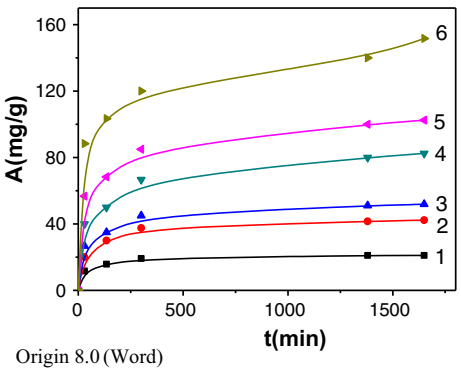

Origin 8.0 (Word)

Fig. 3 Time dependence of DOX adsorption on the surface of Fe_3O_4/HA NC in PS. Initial concentration of DOX solutions C, mg/mL: *1* 0.13, *2* 0.26, *3* 0.32, *4* 0.52, *5* 0.64, *6* 1.04

Distribution coefficient (E, mL/g) of doxorubicin between the surface of nanocomposite and solution was 366.8 mL/g at $A = 91.7$ mg/g.

Upon studies of DOX adsorption on the surface of Fe_3O_4/HA NC as function of time (Fig. 3), it was revealed that during the first 2 h 60–70 % of the substance is adsorbed, and for 24 h the adsorption was almost complete (93–97 %). And this applies to the entire range of the investigated DOX concentrations. The dependence of the extraction extent (R, %) of doxorubicin on concentration of solutions and adsorption time is given in Table 1.

The results of studies on the dependence of desorption (A_D, mg/g) on time and the percentage of desorbed substance (A_D, %) are given in Fig. 4 and Table 2. Experimental dependencies of desorption on time indicate that the doxorubicin release decreases with increasing its quantity on the surface of NC. When the quantity of adsorbed DOX is 20–50 mg/g, 80–60 % of DOX, respectively, is desorbed, whereas at large quantities of adsorbed DOX (100–150 mg/g) the release almost do not occur. This situation can be explained by the peculiarities of interaction and the emergence of sufficiently strong bonds between the

Table 1 Extraction extent of doxorubicin (R) on the surface of Fe_3O_4/HA NC depending on the concentration of solutions and adsorption time (t)

C_0, mg/mL	t, min				
	30	135	300	1380	1620
	R, %				
0.13	53.8	73.1	88.5	97.0	97.0
0.26	46.2	69.2	86.5	95.8	97.7
0.32	50.0	65.6	84.4	95.6	97.2
0.52	46.2	57.7	77.0	92.3	95.2
0.64	53.1	64.0	79.7	93.8	96.1
1.04	49.0	59.6	69.2	80.8	87.5

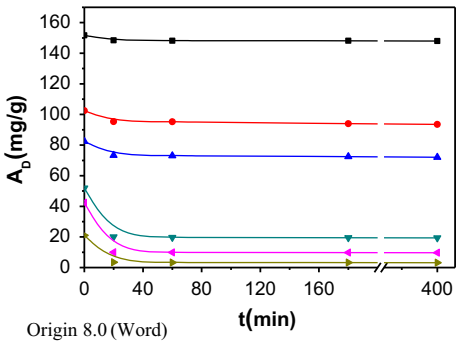

Fig. 4 DOX desorption (A_D) from Fe_3O_4/HA/DOX NC surface in PS *vs* time (t) at different initial amounts of immobilized DOX

Table 2 Dependence of DOX (A_D) desorption from Fe_3O_4/HA/DOX NC surface in PS on time (t) at different initial amounts (A) of immobilized DOX

A, mg/g	t, min			
	20	60	180	400
	A_D, %			
21.0	83.8	84.3	84.3	84.8
42.3	76.4	76.6	76.8	77.0
51.9	61.5	62.1	62.4	62.6
82.5	11.6	11.5	12.1	12.7
102.5	7.0	6.1	8.3	8.7
151.7	2.2	2.3	2.3	2.4

specific functional groups on HA surface and doxorubicin molecules: hydroxyl and carbonate groups of Fe_3O_4/HA NC surface can form strong hydrogen bond with hydroxyl and amino groups of DOX; upon the desorption, in samples with lower concentration of DOX, the drug is desorbed faster through partial dissociation of hydrogen bonds [28].

The basic amount of DOX is desorbed during the first 20 min for all the investigated concentrations.

Biocompatibility and bioactivity of nanocomposites

Biocompatibility of Fe_3O_4/HA NC is a known fact [3–11]. In this paper, biocompatibility and bioactivity of the produced samples was monitored by their effect on viability of baker's yeast *S. cerevisiae* cells [11].

In the study of bioactivity of the original drug doxorubicin, we revealed experimentally that its solution in saline at the concentration of 0.5 mg/mL resulted in almost total death of yeast cells (95 %) for 3.5 days. In the technique for determination of cytotoxicity, it is accepted to use IC_{50} dose at which there is a death of ~50 % of the cells [29]. Therefore, to test bioactivity, a quantity of Fe_3O_4/HA/DOX nanocomposite material (~20 mg) with immobilized doxorubicin (~50 mg/g), that was used to form a suspension, was chosen from the data of Fig. 4 and Table 2 in calculation that the concentration of released DOX in research suspensions was ~0.25 mg/mL.

Fifteen samples in total were investigated, five in each series

1. suspension of yeast cells (initial concentration $n_0 \approx 2.5 \times 10^7$ mL^{-1}) in PS with MSM (Fig. 5a);
2. suspension of yeast cells (initial concentration $n_0 \approx 2.5 \times 10^7$ mL^{-1}) in PS with MSM, containing 20 mg of Fe_3O_4/HA NC;
3. suspension of yeast cells (initial concentration $n_0 \approx 3.5 \times 10^7$ mL^{-1}) in PS with MSM, containing 20 mg of Fe_3O_4/HA/DOX NC.

All the samples contained 1.3 mL of PS (0.9 % NaCl) and 1 mL of MSM. The samples of series 1 and 2 were used for control and comparison, and series 3—for studies on bioactivity of Fe_3O_4/HA/DOX NC.

Research data analysis shows that in the yeast suspensions ($n_0 \approx 2.5 \times 10^7$ mL^{-1}) in the PS with MSM (control series of type 1) there is a characteristic for yeast [30] cell division that leads to an increase in their concentration in 16 h twice (5×10^7 mL^{-1}). Further rate of their reproduction slowed (possibly because of nutrient reduction). In 3.5 days their concentration was ~10^8 mL^{-1}. The viability of yeast cells in the experiments of series 1 was not significantly changed and reached ~98–99 %.

Investigation of suspensions of type 2 control series showed rather active division by which the yeast concentration in 16 h was ~6.5×10^7 mL^{-1}, and in 3.5 days, as in the previous case, reached ~10^8 mL^{-1} (Fig. 5b). Cell viability, as in the previous case, at all stages of the series 2 samples study was ~98–99 %. These data indicate biocompatibility of Fe_3O_4/HA NC with respect to yeast cells under the experiment conditions.

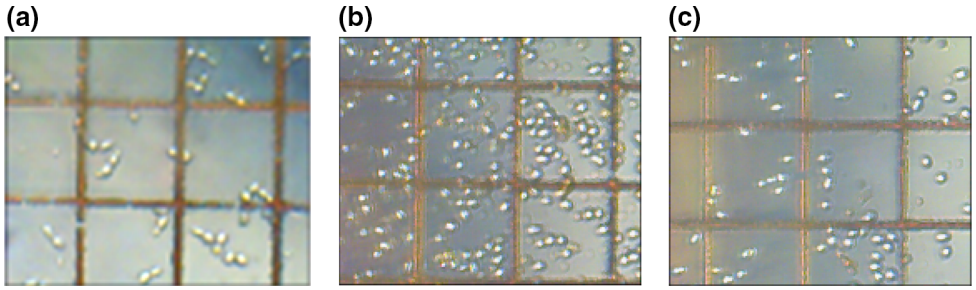

Fig. 5 Typical images of fragments of Goryaev chamber with yeast cells: in beginning of studies (**a**), after interaction of yeast cells with Fe_3O_4/HA NC (**b**), after interaction of yeast cells with Fe_3O_4/HA/DOX NC (**c**). The interaction time is 3.5 days, $T \sim 300$ K, the concentration of cells: **a** 2.5×10^7 mL^{-1}, **b** 1×10^8 mL^{-1}, **c** 3×10^7 mL^{-1}

Upon the studies of series 3 sample suspensions, a significant inhibition of cell proliferation was revealed (Fig. 5c). So, the concentration of yeast cells in the beginning of the experiment was $\sim 3.5 \times 10^7$ mL^{-1} and was practically not changed for 16 h, only in 3.5 days their number increased up to $\sim 4 \times 10^7$ mL^{-1}. During the study, the quantity of dead cells in the samples of series 3 (Fig. 5c) was about 10 %.

Thus, analyzing the results of experiments of series 1 and 2 (Fig. 5b) and comparing them to the data of series 3 (Fig. 5c), we can conclude that Fe_3O_4/HA/DOX nanocomposites have cytotoxic influence on *S. cerevisiae* cells and reduce the rate of their proliferation.

It should be noted that the observed features of magnetosensitive NC Fe_3O_4/HA/DOX influence on yeast cells are characteristic for the interaction of these cells with the free form of doxorubicin [24–26].

Synthesis of magnetic liquids

In the next stage of research, samples of the three types of magnetic liquids based on saline (ML_{1-3}) were synthesized: ML_1 – Fe_3O_4/sodium oleate (Na ol.)/polyethylene glycol (PEG) + PS, ML_2 – Fe_3O_4/HA/Na ol./PEG + PS, ML_3 – Fe_3O_4/HA/DOX/Na ol./PEG + PS. Fe_3O_4 nanoparticles, as well as Fe_3O_4/HA NC and Fe_3O_4/HA/DOX NC particles were stabilized by sodium oleate [31] and polyethylene glycol. It is known that PEG prevents adsorption interactions of components of a liquid with proteins [32], which is important in medical applications of magnetic liquids. For stabilization of the NP and NC surface in the ML composition, the sodium oleate samples of weight m were calculated taking into account the concentration of hydroxyl groups on the surface of magnetite and hydroxyapatite. The calculation was performed using the formula: $m = BMg$, where B is the concentration of hydroxyl groups (2.2 mmol/g on the surface of initial nanosized magnetite and 1.8 mmol/g on the surface of Fe_3O_4/HA nanocomposite, as determined from the data of thermogravimetric analysis using a derivatograph Q–1500), M is the molecular weight of sodium oleate (304 g/mol), g is a sample weight of Fe_3O_4 or NC. Additional modifying with PEG-2000 was carried out in dynamic mode using a shaker; the amount of polymer was 10–15 % of the weight of Fe_3O_4 NP or nanocomposite sample.

Study of magnetic and structural properties of nanocomposites in composition of magnetic liquids

Further researches are based on using the ensemble of superparamagnetic carriers as a probe for determination of parameters and control of nanostructures with complex construction, in particular, in composition of the magnetic liquids [11, 20, 33].

Implementation of the said approach can be achieved using the method of magnetic granulometry [34], based on the comparison of the experimental magnetization curve to Langevin's curve at the given laws of size distribution of particles and their magnetic parameters, including saturation magnetization of the particles and the thickness of "demagnetized layer".

To analyze the magnetization curve of ML containing superparamagnetic nanoparticles, a known equation [35] was applied [11]:

$$\frac{M(H)}{\varphi_\rho M_s} = \frac{\sum_{i=1}^{k} n_i (d_i - 2h_1)^3 L\left(\frac{M_s H}{k_B T}\frac{\pi}{6}(d_i - 2h_1)^3\right)}{\sum_{i=1}^{k} n_i d_i^3}, \quad (1)$$

where M (H) is the magnetization of ML in magnetic field of strength H; M_s is the saturation magnetization of a bulk magnetite; φ_ρ is the volumetric concentration of solid phase in ML, defined by the density of ML; d_i, n_i is the average diameter and quantity of Fe_3O_4 NP in the i interval of the diameter variation row; k is the number of intervals; h_1 is the thickness of "demagnetized layer" of magnetite;

$L(\xi) \equiv cth\xi - 1/\xi$ is the Langevin function; k_B is the Boltzmann constant; T is the temperature.

(a) Determination of the size distribution of ensemble of nanosized magnetite particles and the thickness of their demagnetized layer in terms of the shape of magnetization curves of magnetic liquid.

The ensemble of Fe_3O_4 particles that are characterized by the sizes of 3–23 nm being in superparamagnetic state, has non-hysteresis demagnetization curve, and therefore, zero values of coercive force (H_c) and residual magnetization (M_r) [11]. These features of magnetization are mainly observed in experiment also for samples of ML based on nanocomposites Fe_3O_4/HA/DOX/Na ol./PEG + PS (ML_3) (Fig. 6a).

The specific saturation magnetization σ_s of typical ensembles of Fe_3O_4 NP synthesized for research in this paper was 62.6 ± 2.5 % Gs cm^3/g (Fig. 6b, the upper insertion). In the study of static magnetic characteristics (the measurement time was ~100 s), Fe_3O_4 NP or dry residues (DR) of magnetic liquids were distributed in the matrix of paraffin (to prevent interparticle interaction) under condition $m_{DR}/m_p \sim 0.1$ (m_{DR}—weight of DR, m_p—weight of paraffin). Calculation times of Neel's relaxation of magnetic moment of Fe_3O_4 NP with diameters of 3–22 nm are (10^{-9}–10^2) s, respectively.

According to the experimental curve (Fig. 6a), the coercive force (H_c) of ML_3 is equal to (2 ± 0.5) Oe. The samples of Fe_3O_4 NP and DR_3 of ML_3, distributed in paraffin, are characterized by H_c 89.7 Oe and 90.0 Oe, respectively (Fig. 6b). The availability of coercive force in the investigated samples in a liquid state, probably, is due to the presence of a small number of aggregates, joint by dipole–dipole interaction, and in paraffin matrices—a small number of Fe_3O_4 NP with diameter >22 nm.

The upper insertion in Fig. 6a shows the diameter distribution of Fe_3O_4 NP, obtained in experiment by statistical processing (a program Get Data Graph Digitizer 2.24) of TEM images of initial magnetite (1), and lognormal diameter distribution (2), calculated for the same ensemble using a probability density function, similar to [11]. The average diameter value $d_0 = (\Sigma n_i d_i)/N$ and the standard deviation (s) of diameter of Fe_3O_4 NP for a choice of volume $N = 274$ was 10.77 nm ($s = 3.083$ nm), logarithm of diameter: 2.33 ($s_{\ln d} = 0.298$), logarithm of volume: 6.37 ($s_{\ln V} = 0.894$). For mathematical expectation of Fe_3O_4 particle diameter $M(d)$ and logarithm of diameter $M(\ln d)$, the correlation is just: $M(d) = \exp[M(\ln d) + (\sigma_{\ln d})^2/2]$, where $\sigma_{\ln d}$ is the standard deviation of logarithm of a particle diameter [36]. The value of thickness of "demagnetized" surface layer h_1 of Fe_3O_4 NP, calculated according formula (1) was ~0.83 nm.

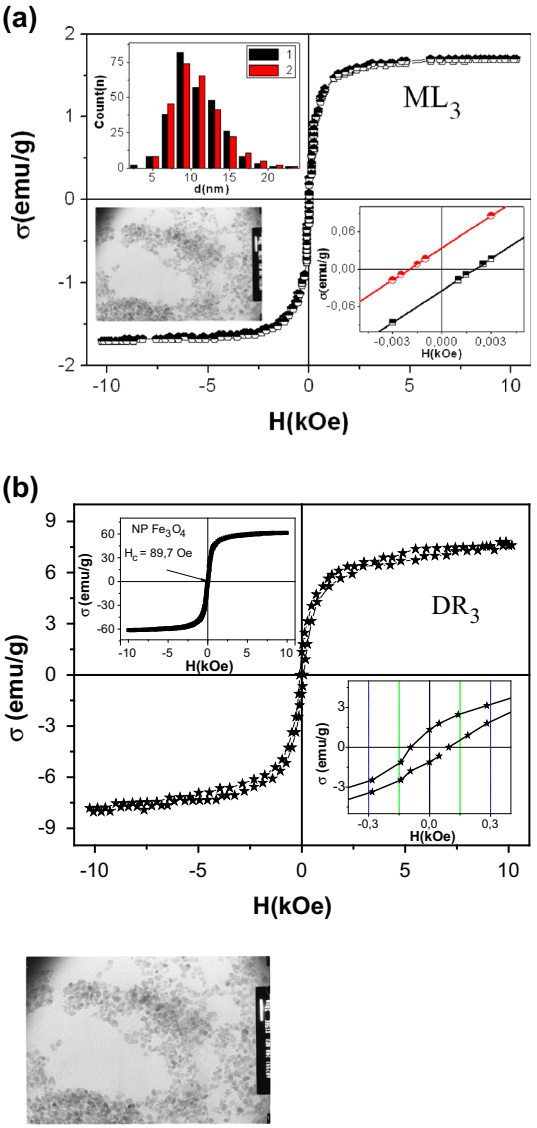

Fig. 6 Hysteresis loops: **a** ML3 (for insertions: the *top 1*, *2*, histograms of experimental and lognormal (2.33, 0.298) distribution of Fe_3O_4 NP by diameters, respectively; the lower ones, TEM images (*scale* 50 nm) of magnetite nanoparticles ensemble and initial part of hysteresis loop of ML3); **b** DR3 in paraffin matrix (for insertions: the *top*, hysteresis loop of Fe_3O_4 NP; the *bottom*, initial part of the loop of DR3)

Figure 7 shows a model of Fe_3O_4/HA/DOX/Na ol./PEG NC particle with a multilayer shell in which: $d = d_s + 2h_1$ is the diameter of a spherical magnetite particle; d_s is the diameter of the area of Fe_3O_4 NP with σ_s which is the characteristic for a bulk magnetite (≈92 emu/g at 300 K); h_1 is the thickness of "demagnetized" layer of Fe_3O_4 particles; h_2, h_3, h_4 are the thickness of spherical layers of modifier (HA), drug (DOX) and stabilizer (Na ol./PEG), respectively.

Using the model (Fig. 7), in terms of the results of experimental measurements and ensemble parameters

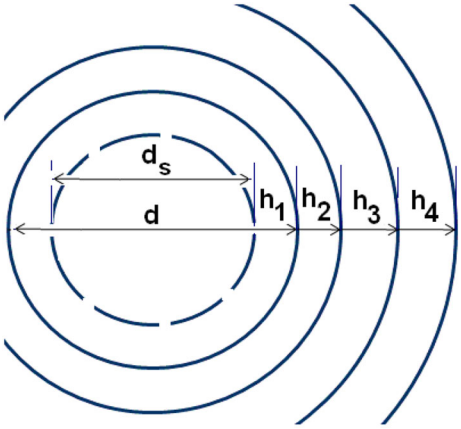

Paint (Word)

Fig. 7 Model of a particle of NC with a multilayer shell. It is marked: $d = d_s + 2h_1$ is the diameter of a spherical Fe_3O_4 NP; d_s is the diameter of the area of Fe_3O_4 NP with σ_s, that is characteristic for a bulk magnetite; h_1 is the thickness of the "demagnetized" surface layer of Fe_3O_4 NP; h_2, h_3, h_4 are the thickness of the modifying layer (HA), drug (DOX), and combined stabilizer (Naol./PEG) in NC structure, respectively

calculation for nanoparticles of magnetite and dry residues of magnetic liquid of corresponding composition, the shell layers sizes of Fe_3O_4/HA/DOX/Na ol./PEG nanostructure were determined.

In [11] it has been shown that for ensembles of nanoparticles of "core–shell" type, under condition of cores to be in a superparamagnetic state, formula (1) practically unequivocally binds the size distribution of Fe_3O_4 NP in ensemble with a shape of hysteresis curve. Taking into account that in conditions of magnetic saturation the Langevin function $L(\xi) \to 1$, and in DR a volumetric concentration of solid phase ~ 1, formula (1) can be written as

$$\frac{M_s^{\mathrm{NCPM}}}{M_s^{\mathrm{NPM}}} = \frac{\langle \rho_{\mathrm{NCPM}} \rangle \sigma_s^{\mathrm{NCPM}} \int_0^\infty V_{\mathrm{NCPM}} f(V_{\mathrm{NCPM}}) \mathrm{d}V}{\langle \rho_{\mathrm{NPM}} \rangle \sigma_s^{\mathrm{NPM}} \int_0^\infty V_{\mathrm{NPM}} f(V_{\mathrm{NPM}}) \mathrm{d}V}, \qquad (2)$$

where M_s^{NCPM}, M_s^{NPM} are the saturation magnetization of ensembles of particles of NC (NCPM) and Fe_3O_4, respectively; $<\rho_{\mathrm{NCPM}}>$, $<\rho_{\mathrm{NPM}}>$ are the average density of ensembles of particles of NC and Fe_3O_4, respectively; σ_s^{NCPM}, σ_s^{NPM} are the specific saturation magnetization of ensembles of particles of NC and Fe_3O_4, respectively; $f(V_{\mathrm{NCPM}})$, $f(V_{\mathrm{NPM}})$ are the probability density functions for the volumes of ensembles of particles of nanocomposite and magnetite, respectively; V_{NCPM}, V_{NPM} are the volume of a particle of NC and Fe_3O_4, respectively.

(b) Determination of thickness of the layer of combined stabilizer (Na ol./PEG)

The synthesized samples of initial Fe_3O_4 and ML_1 composed of Fe_3O_4/Na ol./PEG + PS were dried at room temperature. The mass proportion of magnetite in the dry residue of ML_1 (DR_1) was experimentally defined as $\alpha_{\mathrm{Fe_3O4}}^{\mathrm{exp}} = \sigma_s^{\mathrm{DR1}}/\sigma_s^{\mathrm{NPM}} \pm 5$ %, and calculated by the formula

$$\alpha_{\mathrm{Fe_3O_4}}^{\mathrm{calc}} = \frac{\upsilon_{\mathrm{Fe_3O_4}} \rho_{\mathrm{Fe_3O_4}}}{\langle \rho_{\mathrm{NCPM}} \rangle}, \qquad (3)$$

where $\nu_{\mathrm{Fe3O4}} = \sum n_i d_i^3 / \sum n_i (d_i + 2\delta)^3$ is the volume fraction of magnetite in the sample; $\delta = h_2 + h_3 + h_4$ is the thickness of the shell; ρ_{Fe3O4} is the density of magnetite, $<\rho_{\mathrm{NCPM}}>$ is the average density of the ensemble of NC particles, which was found from the formula

$$\langle \rho_{\mathrm{NCPM}} \rangle = \frac{\sum_{i=1}^{k} n_i \rho_{\mathrm{NCPM}_i} (d_i + 2\delta)^3}{\sum_{i=1}^{k} n_i (d_i + 2\delta)^3} \qquad (4)$$

The density of nanocomposite particles of i interval $\rho_{\mathrm{NCPM}i}$ in composition of DR_{1-3} was determined by formulas (5.1–5.3):

$$\rho_i^{12} = \alpha_2 \rho_1 + (1 - \alpha_2)\rho_2, \text{where } \alpha_2 = \left(\frac{d_i}{d_i + 2h_2} \right)^3, \qquad (5.1)$$

$$\rho_i^{123} = \alpha_3 \rho_i^{12} + (1 - \alpha_3)\rho_3, \text{where } \alpha_3 = \left(\frac{d_i + 2h_2}{d_i + 2h_2 + 2h_3} \right)^3, \qquad (5.2)$$

$$\rho_i^{1234} = \alpha_4 \rho_i^{123} + (1 - \alpha_4)\rho_4, \text{where } \alpha_4 = \left(\frac{d_i + 2h_2 + 2h_3}{d_i + 2h_2 + 2h_3 + 2h_4} \right)^3 \qquad (5.3)$$

and ρ_1, ρ_2, ρ_3, ρ_4 are the density of magnetite, HA, DOX and Na ol./PEG, respectively; ρ_i^{12}, ρ_i^{123}, ρ_i^{1234} are the density of a particle of i interval of NC Fe_3O_4/HA, Fe_3O_4/HA/DOX and Fe_3O_4/HA/DOX/Na ol./PEG, respectively. For calculations, we used the values $\rho_1 \approx 5.19$ g/cm^3 [37], $\rho_2 \approx 2.71$ g/cm^3 [28], $\rho_3 \approx 1.00$ g/cm^3, $\rho_4 \approx 1.13$ g/cm^3 [33]). We considered that the size distribution of Fe_3O_4 NP of the initial ensemble and its dry residues was identical.

Specific surface area of the ensemble of NC particles was determined by the formula

$$S_{\mathrm{sp}}^{\mathrm{calk}} = 6 \frac{\sum_{i=1}^{k} n_i (d_i + 2\delta)^2}{\sum_{i=1}^{k} \rho_{\mathrm{NCPM}_i} (d_i + 2\delta)^3}. \qquad (6)$$

According to the model (Fig. 7) in a particle of DR_1 only h_4 shell is filled (h_2, $h_3 = 0$). The results of experimental measurements and calculations of parameters of ensemble of NP Fe_3O_4 and DR_1 are shown in Table 3.

Table 3 Results of experimental measurements and calculation of parameters of ensemble of NP Fe_3O_4 and DR_1

Experimental values					Calculated values			
Sample	d_0, nm	σ_s, Gs cm^3/g (%)	α^{exp}_{Fe3O4} (%)	S^{exp}_{sp}, m^2/g (%)	h_4, nm	$<\rho_{NCPM}>$, g/cm^3 (%)	α^{calc}_{Fe3O4}	S^{cal}_{sp}, m^2/g
Fe_3O_4	10.8	62.6 ± 2.5	1.00 ± 5	107.0 ± 5	0	5.19 ± 1	1.00	107.0
DR_1	10.8	36.6 ± 2.5	0.58 ± 5	161.0 ± 5	3.4 ± 3	2.07 ± 1	0.58	161.0

The value of $<\rho_{NCPM}>$ was calculated by formulas (4)–(5.1–5.3), α^{calc}_{Fe3O4}—by formula (3). h_4 value was found, at which $\alpha^{calc}_{Fe3O4} = \alpha^{exp}_{Fe3O4}$. In terms of the obtained h_4 and formulas (5.1–5.3)–(6), S^{calc}_{sp} was determined

As shown in Table 3, thickness of the shell of combined stabilizer Na ol./PEG in composition of dry residue of magnetic liquid Fe_3O_4/Na ol./PEG + PS is (3.4 ± 0.1) nm.

(c) Determination of the thickness of HA layer

To determine the thickness of HA layer we studied the ensemble of NP Fe_3O_4 and ML_2 composed of Fe_3O_4/HA/Na ol./PEG + PS obtained on its basis, the samples were dried at room temperature, dry residue DR_2 was obtained and their parameters were investigated by the technique described above. The results are shown in Table 4.

As shown in Table 4, the found value of thickness of hydroxyapatite layer h_2 in the structure of Fe_3O_4/HA/Na ol./PEG is 3.5 ± 0.3 nm, which in our view is satisfactorily consistent with the value of ~4 nm, determined by an independent technique in studies of Fe_3O_4/HA nanocomposites by photoelectron spectroscopy method [11]. The obtained data may indicate reliability of the results of determination of shell parameters in complex nanoarchitecture of multifunctional magnetosensitive nanocomposites.

(d) Determination of the thickness of DOX layer

The ensemble of magnetite nanoparticles and ML_3 composed of Fe_3O_4/HA/DOX/Na ol./PEG + PS obtained on their basis, were dried at room temperature. The dried samples Fe_3O_4 and dry residue DR_3 were studied, as in the previous cases. The research results are given in Table 5.

According to the data of Table 5, the found value of thickness of the layer of medical drug doxorubicin h_3 in the structure of Fe_3O_4/HA/DOX/Na ol./PEG is 2.0 ± 0.3 nm.

(e) Study of sedimentation stability of magnetic liquids

The investigated ML are nanoheterogeneous systems, where diffusion fluxes of particles dominate over sedimentation ones. Over a long period of time (years) in monodisperse sols, the fluxes become equal and a state of diffusion-sedimentation equilibrium (DSE) is set, at which the distribution of particles on height of a vessel is subjected to the hypsometric law [37]:

$$\nu_h/\nu_0 = \exp\left[-\frac{V_{cp}(\rho_{cp} - \rho_{lc})gh}{k_BT}\right], \quad (7)$$

where ν_h, ν_0 are the concentrations of particles at height h and at the level of bottom of a vessel, respectively; V_{cp}, ρ_{cp} are the volume and density of colloidal particles, respectively; ρ_{lc} is the density of a liquid carrier; g is the acceleration of gravity.

The height at which concentration of particles varies in e times, characterizes the thermodynamic sedimentation stability (TDS) of a colloidal system [37] (hypsometric height L). From Eq. (7) it follows that

$$L = \frac{k_BT}{V_{cp}(\rho_{cp} - \rho_{lc})g} = \frac{6k_BT}{\pi(d + 2\delta)^3(\langle\rho_{NCPM}\rangle - \rho_{lc})g}, \quad (8)$$

where $<\rho_{NCPM}>$ is the mean density of a nanocomposite particle with diameter of core d and thickness of shell δ, calculated by formulas (5.1–5.3).

In polydisperse systems, DSE is set for each fraction of particles. Time of setting DSE (t_b) in ML was calculated by the technique given in [33]: we used formula $t_b = L_0^2/<D>$, where $<D> = (1/N)\sum k_BT/[3\pi\eta(d_i + 2\delta)]$ is the average diffusion coefficient; $L_0 = k_BT/[<V_{NCPM}>\ (<\rho_{NCPM}> - \rho_{lc})g]$ is the average hypsometric height; η is the dynamic viscosity, determined for the concentrated ML by a laboratory viscometer (the time of leakage of the fluid through a glass capillar with diameter of 0.2 mm was ≈300 s); the value η of diluted ML, according to experimental data [18], was calculated by Einstein formula: $\eta/\eta_0 = 1 + 5\varphi/2$, where η_0 is the dynamic viscosity of the liquid carrier (η_0 of PS is approximately equal to 0.890 mPa s at the

Table 4 Results of experimental measurements and calculation of parameters of ensemble of NP Fe_3O_4 and DR_2

Sample	Experimental values				Calculated values				
	d_0, nm	σ_s, Gs cm^3/g (%)	α^{exp}_{Fe3O4} (%)	S^{exp}_{sp}, m^2/g (%)	h_2, nm	h_4, nm	$<\rho_{NCPM}>$, g/cm^3 (%)	α^{calc}_{Fe3O4}	S^{cal}_{sp}, m^2/g
Fe_3O_4	10.8	62.6 ± 2.5	1.00 ± 5	107.0 ± 5	0	0	5.19 ± 1	1.00	107.0
DR_2	10.8	13.2 ± 2.5	0.21 ± 5	114.0 ± 5	3.5 ± 3	3.4 ± 3	2.07 ± 1	0.20	114.6

Table 5 Results of experimental measurements and calculation of parameters of magnetite nanoparticles ensemble and dry ML3 residues

Experimental values					Calculated values					
Sample	d_0, nm	σ_s, Gs cm^3/g (%)	α^{exp}_{Fe3O4} (%)	S^{exp}_{sp}, m^2/g (%)	h_2, nm (%)	h_3, nm (%)	h_4, nm (%)	$<\rho_{NCPM}>$, g/cm^3 (%)	α^{calc}_{Fe3O4}	S^{cal}_{sp}, m^2/g
Fe_3O_4	10.8	62.6 ± 2.5	1.00 ± 5	107 ± 3	0	0	0	5.19 ± 1	1.00	107.0
DR_3	10.8	9.9 ± 2.5	0.16 ± 5	120 ± 3	3.5 ± 3	2.0 ± 3	3.4 ± 3	1.74 ± 1	0.15	120.1

temperature of 25 °C). The estimated values t_b in ML_{1-3} are nine years and more. The experimental value of L for ML_3 is $L^{exp} = 2.4 \pm 8$ % cm.

Using the found parameters of Fe_3O_4/HA/DOX/Na ol./PEG nanostructure in composition of magnetic liquid, the dependencies of hypsometric height (Fig. 8, curve 1) and specific surface area of DR (curve 2) on thickness h_3 of DOX layer were plotted for the model magnetic liquid of ML_3 type, in which Fe_3O_4/HA/DOX/Na ol./PEG NC was characterized by the fixed size of the core and layers of hydroxyapatite and combined stabilizer ($d_{Fe3O4\ NP} = 10.8$ nm, $h_2 = 3.5$ nm, $h_4 = 3.4$ nm). Calculation dependence $L(h_3)$ was built by formula (8), $S_{sp}(h_3)$—(9):

$$S_{sp} = \frac{6}{\rho_{NCPM}(d + 2\delta)} \quad (9)$$

The value $<\rho_{NCPM}>$ was obtained by the formulas (5.1–5.3).

Dependence $L(h_3)$, shown in Fig. 8, curve 1, is typical for the colloidal systems [37]. The experimental value of L for ML_3 ($L^{exp} = 2.4 \pm 8$ % cm) corresponds to $h_3 = 2.2 \pm 8$ % nm.

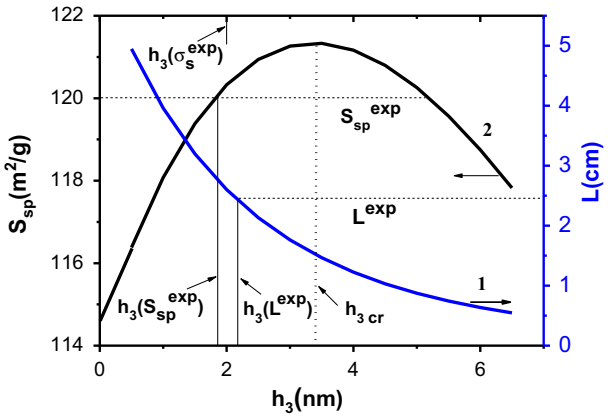

Origin 8.0 (Word)

Fig. 8 Calculation dependences: hypsometric height L (*curve 1*) and specific surface area *Ssp* of DR (*curve 2*) on the thickness *h*3 of DOX layer for the model magnetic liquid of ML3 type, in which Fe_3O_4/HA/DOX/Na ol./PEG NC is characterized by the fixed size of the core and layers of hydroxyapatite and combined stabilizer (dFe_3O_4 NP = 10.8 nm, $h_2 = 3.5$ nm, $h_4 = 3.4$ nm)

Dependence $S_{sp}(h_3)$ given in Fig. 8 (curve 2) has a maximum caused by that S_{sp} is a complex function of ρ_{NCPM} and $(d + 2\delta)$. Its position (h_{3cr}) can be found analytically by equating to zero the expression $dS_{sp}/d\delta$ (the criterion for finding thickness of the shell, which corresponds to the maximal specific surface area of the core–shell structure S_{sp}). Ordinate corresponding to the experimental value $S^{exp}_{sp} = 120 \pm 3$ % for DR_3 (Table 5), twice crosses the calculated dependence S_{sp} with abscissas $h_3 = 1.94$ nm and $h_3 = 5.0$ nm. The value $h_3 = 5.0$ nm contradicts the data of magnetic measurements (Table 5) and the value obtained by L^{exp} (Fig. 8, curve 1).

So, using three independent experimental methods for measurement of σ_s, L, S_{sp}, we obtained three values of the thickness of doxorubicin layer h_3 in the structure of Fe_3O_4/HA/DOX nanocomposite: 2.0 nm (Table 5), 2.2 nm (Fig. 8, curve 1), 1.94 nm (Fig. 8, curve 2), respectively. The found values h_3 are rather close, which shows their reliability.

We note that analysis of the sizes of superparamagnetic iron oxide nanoparticles coated with a layer of carboxydextran, which are applied as contrast agents in magnetic resonance imaging (a commercial product Resovist and SH U555C) using a magnetization curve and images of ensembles of particles, obtained by transmission electron microscopy, has been performed in [38].

The results of experimental investigations and calculations given in this paper, their testing by different ways and comparison suggest that using ensembles of magnetic carriers as a superparamagnetic probe and Langevin's paramagnetism theory, one can evaluate the sizes of the components of complex shell structure of nanocomposites. The obtained data may be useful in optimizing chemical composition, structure and properties of new magnetic liquids and adsorbents containing magnetosensitive nanocomposites with complex construction of shell [39, 40].

Conclusions

The processes of DOX adsorption on Fe_3O_4/HA NC surface from solution in physiologic liquid were studied. It was determined that an increase in equilibrium

concentration of DOX within the studied concentration range does not lead to adsorption saturation of the surface of Fe_3O_4/HA adsorbent. It was revealed that release of DOX into saline decreases with growing of its quantity on NC surface.

Magnetosensitive Fe_3O_4/HA/DOX NC were synthesized. It has been determined that cytotoxic influence and antiproliferative activity of NC with respect to *S. cerevisiae* cells are typical for interaction of these cells with a free form of doxorubicin.

Magnetic liquids containing Fe_3O_4/HA/DOX NC stabilized by sodium oleate and polyethylene glycol were produced and investigated. Using the ensemble of Fe_3O_4 carriers as a superparamagnetic probe, Langevin's paramagnetism theory, the values of density of nanocomposite constituents, the size parameters of their shell were evaluated, which was corroborated by independent measurements of specific surface area of nanostructures and kinetic stability of the corresponding magnetic liquids. The obtained results may be used for the development of novel forms of magnetocarried medical remedies for targeted delivery and adsorbents based on nanocomposites of superparamagnetic core–shell type with multilevel nanoarchitecture, as well as for determination, control, and optimization of the size parameters of its components.

Acknowledgments The work was carried out with support of goal complex programs of fundamental investigations of the National Academy of Sciences of Ukraine "Fine Chemicals" (project 31/16) and "Fundamental problems in creation of novel nanomaterials and nanotechnologies" (project 38/16-N).

Compliance with ethical standards

Conflict of interest The authors declare that they have no competing interests.

References

1. Roco M.C., Williams, R.S., Alivisatos, P.: Vision for Nanotechnology R&D in the Next Decade. Kluwer Academic, Dordrecht. http://www.wtec.org/loyola/nano/IWGN.Research.Directions/IWGN_rd.pdf (2002)
2. Levy, L., Sahoo, Y., Kim, K.-S., Bergey, J.E., Prasad, P.: Synthesis and characterization of multifunctional nanoclinics for biological applications. Chem. Mater. **14**, 3715–3721. http://pubs.acs.org/doi/abs/10.1021/cm0203013 (2002)
3. Gorbyk, P.P., Dubrovin, I.V., Petranovska, A.L., Abramov, M.V., Usov, D.G., Storozhuk, L.P., Turanska, S.P., Turelyk, M.P., Chekhun, V.F., Lukyanova, N.Y., Shpak, A.P., Korduban, O.M.: Chemical construction of polyfunctional nanocomposites and nanorobots for medico-biological applications. In: Shpak, A.P., Gorbyk, P.P. (eds.) Nanomaterials and Supramolecular Structures. Physics, Chemistry, and Applications, pp. 63–78. Naukova dumka, Springer, Kiev. http://www.springer.com/us/book/9789048123087(2009)
4. Gorbyk, P.P., Chekhun, V.F.: Nanocomposites of medicobiologic destination: reality and perspectives for oncology. Funct. Mater. **19**(2), 145–156. http://functmaterials.org.ua/contents/19-2/fm192-01.pdf (2012)
5. Gorbyk, P.P., Lerman, L.B., Petranovska, A.L., Turanska, S.P.: Magnetosensitive nanocomposites with functions of medico-biological nanorobots: synthesis and properties. In: Adorno, D.P., Pokutnyi, S. (eds.) Advances in Semiconductor Research: Physics of Nanosystems, Spintronics and Technological Applications, pp. 161–198. Nova Science Publishers, N. Y. www.novapublishers.com/catalog/product_info.php?products_id=51113 (2014)
6. Huang, C., Zhou, Y., Tang, Z., Guo, X., Qian, Z., Zhou, S.: Synthesis of multifunctional Fe_3O_4 core/hydroxyapatite shell nanocomposites by biomineralization. Dalton Trans. **40**(18), 5026–5031. http://www.ncbi.nlm.nih.gov/pubmed/21455509 (2011)
7. Iwasaki, T.: Mechanochemical synthesis of magnetite/hydroxyapatite nanocomposites for hyperthermia. In: Mastai, Y. (ed.) Materials Science—Advanced Topics, pp. 175–194. InTech (2013). doi:10.5772/54344
8. Gopi, D., Ansari, M.T., Shinyjoy, E., Kavitha, L.: Synthesis and spectroscopic characterization of magnetic hydroxyapatite nanocomposite using ultrasonic irradiation. Spectrochimica Acta Part A Mol. Biomol. Spectrosc. **87**, 245–250. http://www.sciencedirect.com/science/article/pii/S1386142511010420 (2012)
9. Mir, A., Mallik, D., Bhattacharyya, S., Mahata, D., Sinha, A., Nayar, S.: Aqueous ferrofluids as templates for magnetic hydroxyapatite nanocomposites. Aqueous ferrofluids as templates for magnetic hydroxyapatite nanocomposites. J. Mater. Sci: Mater. Med. **21**, 2365–2369. http://www.researchgate.net/publication/44633635_Aqueous_ferrofluids_as_templates_for_magnetic_hydroxyapatite_nanocomposites (2010)
10. Feng, C., Chao, L., Ying-Jie, Z., Xin-Yu, Z., Bing-Qiang, L., Jin, W.: Magnetic nanocomposite of hydroxyapatite ultrathin nanosheets/Fe_3O_4 nanoparticles: microwave-assisted rapid synthesis and application in pH-responsive drug release. Biomater. Sci. **1**, 1074–1081. http://pubs.rsc.org/en/content/articlelanding/2013/bm/c3bm60086f/unauth#!divAbstract (2013)
11. Petranovska, A.L., Abramov, N.V., Turanska, S.P., Gorbyk, P.P., Kaminskiy, A.N., Kusyak, N.V.: Adsorption of *cis*-dichlorodiammineplatinum by nanostructures based on single-domain magnetite. J. Nanostruct. Chem. **5**, 275–285. http://link.springer.com/article/10.1007/s40097-015-0159-9?wt_mc=alerts.TOCjournals (2015)
12. Petranovska, A.L., Turelik, M.P., Pylypchuk, I.V., Gorbyk, P.P., Korduban, A.M., Ivasishin, O.M.: Formirovaniye biomimetich-eskogo gidroksiapatita na poverkhnosti titana. Metallofizika i Noveishyye Tekhnologii. **35**(11), 1567–1584. http://mfint.imp.kiev.ua/ru/toc/v35/i11.html (2013)
13. Pylypchuk, I.V., Petranovska, A.L., Turelyk, M.P., Gorbyk, P.P.: Formation of biomimetic hydroxyapatite coating on titanium plates. Mat. Science (Med.) **20**(3), 328–332 (2014). doi:10.5755/j01.ms.20.3.4974
14. Pylypchuk, I.V., Petranovska, A.L., Gorbyk, P.P., Korduban, A.M., Markovsky, P.E., Ivasishin, O.M.: Biomimetic hydroxyapatite growth on functionalized surfaces of Ti-6Al-4 V and Ti-Zr-Nb alloys. Nanoscale Res. Lett. **10**, 338. http://www.nanoscaleresletters.com/content/10/1/338/abstract (2015)
15. Davaran, S., Alimirzalu, S., Nejati-Koshki, K., Nasrabadi, H.T., Akbarzadeh, A., Khandaghi, A.A., Abbasian,

M., Alimohammadi, S.: Physicochemical characteristics of Fe_3O_4 magnetic nanocomposites based on poly(N-isopropylacrylamide) for anti-cancer drug delivery. Asian Pac. J. Cancer Prev. **15**(1), 49–54. http://www.apjcpcontrol.org/paper_file/issue_abs/Volume15_No1/49-54%208.14%20Soodabeh%20Davaran.pdf (2014)
16. Anirudhan, T.S., Sandeep, S.: Synthesis, characterization, cellular uptake and cytotoxicity of a multi-functional magnetic nanocomposite for the targeted delivery and controlled release of doxorubicin to cancer cells. J. Mater. Chem. **22**, 12888–12899. http://pubs.rsc.org/en/Content/ArticleLanding/2012/JM/C2JM31794J#!divAbstract (2012)
17. Sadighian, S., Hosseini-Monfared, H., Rostamizadeh, K., Hamidi, M.: pH-Triggered magnetic-chitosan Nanogels (MCNs) for doxorubicin delivery: physically vs. chemically cross linking approach. Adv. Pharm. Bull. **5**(1), 115–120. http://journals.tbzmed.ac.ir/APB/Manuscript/APB-5-115.pdf (2015)
18. Rozentsveyg, R.: Ferrogidrodinamika. Mir, Moskva. http://www.twirpx.com/file/179455/ (1989)
19. Araújo-Neto, R.P., Silva-Freitas, E.L., Carvalho, J.F., Pontes, T.R.F., Silva, K.L., Damasceno, I.H.M., Egito, E.S.T., Dantas, A.L., Morales, M.A., Carriço, A.S.: Monodisperse sodium oleate coated magnetite high susceptibility nanoparticles for hyperthermia applications. J. Magn. Magn. Mater. **364**, 72–79. http://www.sciencedirect.com/science/journal/03048853/364 (2014)
20. Abramov, N.V., Gorbyk, P.P.: Svoystva ansambley nanochastits magnetita i magnitnykh zhydkostey dlya primeneniy v onkoterapii. Poverkhnost'. **4**(19), 246 http://surfacezbir.com.ua/images/Arhiv/N19/3/3-8Abramov246-265.pdf (2012)
21. Borisenko, N.V., Bogatyrev, V.M., Dubrovin, I.V., Abramov, N.V., Gayevaya, M.V., Gorbyk, P.P.: Sintez i svoistva magnitochuvstvitel'nykh nanokompositov na osnove oksidov zheleza i kremniya. In: Shpak, A.P., Gorbyk, P.P. (eds.) Fiziko-khimiya Nanomaterialov i Supramolekulyarnykh Struktur. **1**, pp. 394–406. Naukova dumka, Kiev. http://www.irbis-nbuv.gov.ua/cgi-bin/irbis_nbuv/ (2007)
22. Turov, V.V., Gorbik, S.P.: Opredeleniye sil adgezii na mezhfaznoy granize kletka/voda iz dannykh ^{1}H YMR spektroskopii. Ukrainskiy Khimicheskiy Zhurnal. **69**(6), 80–85 (2003)
23. Turov, V.V., Gorbik, S.P., Chuiko, A.A.: Vliyaniye dispersnogo kremnezema na svyazannuyu vodu v zamorozhennykh kletochnykh suspenziyakh. Problemy Kriobiologii. **3**, 16–23 (2002)
24. Saenko, Y.V., Shutov, A.M., Rastorgueva, E.V.: Doxorubicin i menadion vyzyvayut zaderzhku kletochnoy proliferacii *Saccharomyces cerevisiae* s pomoshchyu razlichnykh mekhanizmov. Citologiya. **52**(5), 407–411. http://www.tsitologiya.cytspb.rssi.ru/52_5/saenko.pdf (2010)
25. Huang, R.Y., Kowalski, D., Minderman, H., Gandhi, N., Johnson, E.S.: Small ubiquitin-related modifier pathway is a major determinant of doxorubicin cytotoxicity in Saccharomyces cerevisiae. Cancer Res. **67**(2), 765–772. http://www.pubfacts.com/detail/17234788/Small-ubiquitin-related-modifier-pathway-is-a-major-determinant-of-doxorubicin-cytotoxicity-in-Sacch (2007)
26. Patel, S., Sprung, A.U., Keller, B.A., Heaton, V.J., Fisher, L.M.: Identification of yeast DNA topoisomerase II mutants resistant to the antitumor drug doxorubicin: implications for the mechanisms of doxorubicin action and cytotoxicity. Mol. Pharmacol. **52**(4), 658–666. http://www.ncbi.nlm.nih.gov/pubmed/9380029 (1997)
27. Tacar, O., Sriamornsak, P., Dass, C.R.: Doxorubicin: an update on anticancer molecular action, toxicity and novel drug delivery systems. J. Pharm. Pharmacol. **65**(2): 157–170 (2013). doi:10.1111/j.2042-7158.2012.01567.x
28. Biswanath, K., Debasree, G., Mithlesh, K.S., Partha, S.S., Vamsi, K.B., Nirmalendu, D., Debabrata, B.: Doxorubicin-intercalated nano-hydroxyapatite drug-delivery system for liver cancer: an animal model. Ceram. Int. **39**(8), 9557–9566. http://www.sciencedirect.com/science/article/pii/S0272884213005890 (2013)
29. Shpak, A.P., Chekhun, V.F., Gorbyk, P.P., Turov, V.V.: Nanomaterialy i Nanokompozity v Medizyne, Biologii, Ekologii. Naukova dumka, Kiev. http://www.irbis-nbuv.gov.ua/ (2011)
30. Babyeva, I.P., Chernov, I.Y.: Biologiya Drozhzhey. T-vo nauch. izd. KMK, Moskva. http://ashipunov.info/shipunov/school/books/babjeva2004_biologija_drozhzhej.pdf (2004)
31. Sun, S., Zeng, H., Robinson, D.B.: Monodispersed MFe2O4 (M = Fe, Co, Mn) nanoparticles. J. Am. Chem. Soc. **126**, 73–279. http://www.researchgate.net/publication/8931334_Monodisperse_MFe2O4_(M__Fe_Co_Mn)_nanoparticles (2004)
32. Mornet, S., Vasseur, S., Grasset, F., Veverka, P., Goglio, G., Demourgues, A., Portier, J., Pollert, E., Duguet, E.: Magnetic nanoparticle design for medical applications. Prog. Sol. St. Chem. **34**, 237–247. http://science.report/author/s-mornet/ (2006)
33. Abramov, N.V.: Magnitnyye zhidkosti na osnove doxorubicina dlya primeneniy v onkoterapii. Poverkhnost'. **6**, 241–258. http://surfacezbir.com.ua/images/Arhiv/N21/20.3.7.pdf (2014)
34. Banerjee, S.K., Moskowitz, B.M.: Ferrimagnetic properties of magnetite. In: Kirschvink, J.L., Jones, D.S., MacFadden, B.J. (eds.) Magnetite Biomineralization and Magnetoreception in Organisms (1st Edition). A New Biomagnetism (Topics in Geobiology). **5**, pp. 17–41. Plenum Press, New York. http://link.springer.com/chapter/10.1007/978-1-4613-0313-8_2 (1985)
35. Kim, T., Shima, M.: Reduced magnetization in magnetic oxide nanoparticles. J. Appl. Phys. **101,** 09M516. http://connection.ebscohost.com/c/articles/25114951/reduced-magnetization-magnetic-oxide-nanoparticles (2007)
36. Sahoo, P.: Probability and Mathematical Statistics. University of Louisville, Louisville. http://www.math.louisville.edu/~pksaho01/teaching/Math662TB-09S.pdf (2008)
37. Frolov, Y.G.: Kurs Kolloidnoy Khimii. Khimiya, Moskva http://t-library.org.ua/showBook.php?id=3276 (1989)
38. Chen, D.-X., Sun, N., Gu, H.-C.: Size analysis of carboxydextran coated superparamagnetic iron oxide particles used as contrast agents of magnetic resonance imaging. J. App. Phys. **106**(6), 063906–063906-9 http://dx.doi.org/10.1063/1.3211307 (2009)
39. Pokutnyi, S.I.: Theory of excitons and quasimolecules formed from spatially separated electrons and holes in quasi-zero-dimensional semiconductor nanosystems. In: Adorno, D.P., Pokutnyi, S.I. (eds.) Advances in Semiconductor Research: Physics of Nanosystems, Spintronics and Technological Applications, pp. 73–90. Nova Science Publishers, New York. http://www.amazon.com/Advances-Semiconductor-Research-Technological-Applications/dp/1633217558 (2014)
40. Gorbyk, P.P., Lerman, L.B., Petranovska, A.L., Turanska, S.P., Pylypchuk, I.V.: Magnetosensitive nanocomposites with hierarchical nanoarchitecture as biomedical nanorobots: synthesis, properties, and application. In: Grumezescu, A. (ed.) Fabrication and Self-assembly of Nanobiomaterials, Applications of Nanobiomaterials, pp. 289–334. William Andrew, Elsevier. http://store.elsevier.com/product.jsp? (2016)